WHY SO PESSIMISTIC? ESTIMATING UNCERTAINTIES FOR OFFLINE RL THROUGH ENSEMBLES, AND WHY THEIR INDEPENDENCE MATTERS.

Anonymous authors
Paper under double-blind review

ABSTRACT

In order to achieve strong performance in offline reinforcement learning (RL), it is necessary to act conservatively with respect to confident lower-bounds on anticipated values of actions. Thus, a valuable approach would be to obtain high quality uncertainty estimates on action values. In current supervised learning literature, state-of-the-art approaches to uncertainty estimation and calibration rely on ensembling methods. In this work, we aim to transfer the success of ensembles from supervised learning to the setting of batch RL. We propose, MSG, a model-free dynamic programming based offline RL method that trains an ensemble of independent Q-functions, and updates a policy to act conservatively with respect to the uncertainties derived from the ensemble. Theoretically, by referring to the literature on infinite-width neural networks, we demonstrate the crucial dependence of the quality of uncertainty on the manner in which ensembling is performed, a phenomenon that arises due to the dynamic programming nature of RL and overlooked by existing offline RL methods. Our theoretical predictions are corroborated by pedagogical examples on toy MDPs, as well as empirical comparisons in benchmark continuous control domains. In the more challenging domains of the D4RL offline RL benchmark, MSG significantly surpasses highly well-tuned state-of-the-art methods in batch RL. Motivated by the success of MSG, we investigate whether efficient approximations to ensembles can be as effective. We demonstrate that while efficient variants outperform current state-of-the-art, they do not match MSG with deep ensembles. We hope our work engenders increased focus into deep network uncertainty estimation techniques directed for reinforcement learning.

1 INTRODUCTION

Offline Reinforcement Learning (RL), also referred to as Batch RL, is the setting where we are provided with a dataset of interactions with a Markov Decision Process (MDP), and the goal is to learn an effective policy without further interactions with the MDP. Offline RL holds the promise of data-efficiency through data reuse and improved safety due to minimizing the need for policy rollouts. As a result, Batch RL has been a subject of significant renewed interest in the machine learning literature (Levine et al., 2020).

One of the most popular frameworks for offline RL is the model-free setting, using value estimation through approximate dynamic programming (ADP). The predominant algorithmic philosophy with most success in ADP-based offline RL is to limit obtained policies to the support set of the available offline data, with the intuition being that such constraints would reduce inaccurate value estimates since the actions chosen by the policy are close to the observed data. A large variety of methods have been developed for enforcing such constraints, examples of which include: regularizing policies with behavior cloning objectives (Kumar et al., 2019; Fujimoto & Gu, 2021; **?**), only performing updates on actions observed in (Peng et al., 2019; Nair et al., 2020; Wang et al., 2020; Ghasemipour et al., 2021) or close to (Fujimoto et al., 2019) the offline dataset, and regularizing to lower the estimated value of actions not seen in the dataset (Wu et al., 2019; Kumar et al., 2020).

Support constraint forms of regularization correspond to a very pessimistic assumption that any action outside the provided data can lead to a very negative outcome (Buckman et al., 2020). Instead,

it would be preferable if we could place more trust into the predictions of value networks beyond the training dataset. Indeed in adjacent fields of A.I., for different tasks of interest, researchers have spent significant effort developing architectures with built-in inductive biases to help neural networks not only obtain strong accuracy on the training set, but perform well beyond the data they were trained on: convolutional and residual networks for computer vision (He et al., 2016), recurrent networks and transformers for NLP (Vaswani et al., 2017), graph neural networks for graph-based data (Li et al., 2015), and Nerf and Siren for effective signal modelling (Sitzmann et al., 2020; Mildenhall et al., 2020).

However, trusting the predictions of neural networks beyond the training data is a challenging ordeal. Many works have demonstrated that neural networks are prone to making high-confidence incorrect predictions outside the training set, even on i.i.d. test data(Guo et al., 2017). This is a particularly major issue for value estimation, since errors rapidly accumulate through dynamic programming and lead to catastrophic results. Thus, in order to trust our models beyond the training set, it is critical to obtain high quality uncertainty estimates on predicted action values.

In current supervised learning literature, "Deep Ensembles" and their more efficient variants have been shown to be the most effective method for uncertainty estimation (Ovadia et al., 2019). In this work, we aim to transfer the success of ensembles for uncertainty estimation to the setting of batch RL. We begin by presenting MSG, an actor-critic offline RL algorithm leveraging an ensemble of Q-value functions. MSG trains N Q-value functions completely independent of one-another, and updates an actor network with respect to a lower confidence bound (LCB) on action values, obtained from the ensemble. By referring to the literature of infinite-width neural networks, we theoretically demonstrate the critical importance of independence in Q-functions, a deviation from standard practice in RL. Our theoretical predictions are corroborated by experiments in a toy MDP, and their relevance to practical settings is also verified through benchmark experiments.

In established benchmarks for offline RL, we demonstrate that MSG matches, and in the more challenging domains, significantly exceeds the prior state-of-the-art. Inspired by this success, we investigate whether the performance of MSG can be recovered through modern efficient approaches to ensembling. While we demonstrate that efficient ensembles continue to outperform current state-of-the-art batch RL algorithms, they cannot recover the performance of MSG using full deep ensembles.

We hope that our work highlights some of the unique challenges of uncertainty estimation in reinforcement learning, and the significant impact it can have on the performance of algorithms. We also hope that our work encourages stronger engagement from researchers specializing in uncertainty estimation techniques – who typically use computer vision and NLP tasks as benchmarks – to use offline RL as an additional testbed. Due to the rapid accumulation of errors, offline RL can be a pedagogical and challenging testbed for uncertainty estimation research.

2 Related Work

Uncertainty estimation is a core component of RL, since an agent only has a limited view into the mechanics of the environment through its available experience data. Traditionally, uncertainty estimation has been key to developing proper *exploration* strategies such as upper confidence bound (UCB) and Thompson sampling (Lattimore & Szepesvári, 2020), in which an agent is encouraged to seek out paths where its uncertainty is high. Offline RL presents an alternative paradigm, where the agent must act conservatively and is thus encouraged to seek out paths where its uncertainty is low (Buckman et al., 2020). In either case, proper and accurate estimation of uncertainties is paramount. To this end, much research has been produced towards the end of devising provably correct uncertainty estimates (Thomas et al., 2015; Feng et al., 2020; Dai et al., 2020), or, at least, bounds on uncertainty that are good enough for acting either exploratory (Strehl et al., 2009) or conservatively (Kuzborskij et al., 2021). However, these approaches require exceedingly simple environment structure, typically either a finite discrete state and action space or linear spaces with linear dynamics and rewards.

Theoretical guarantees for uncertainty estimation is more limited in practical situations with deep neural network function approximators. Nevertheless, a number of works have been able to achieve practical success, for example using deep network analogues for count-based uncertainty (Ostrovski

et al., 2017), Bayesian uncertainty (Ghavamzadeh et al., 2016; Yang et al., 2020), and bootstrapping (Osband et al., 2019; Kostrikov & Nachum, 2020). Many of these methods employ ensembles. In fact, in continuous control RL, it is common to use an ensemble of two value functions and use their minimum for computing a target value during Bellman error minimization (Fujimoto et al., 2018). A number of works in offline RL have extended this to propose backing up minimums or lower confidence bound estimates over larger ensembles (Kumar et al., 2019; Wu et al., 2019; Agarwal et al., 2020). In our work, we continue to find that ensembles are extremely useful for acting conservatively, but the manner in which ensembles are used is critical. Specifically our proposed MSG algorithm advocates for using independently learned ensembles, without sharing of target values.

The widespread success of ensembles for uncertainty estimation echoes similar findings in supervised deep learning. While there exist proposals for more technical approaches to uncertainty estimation (Li et al., 2007; Neal, 2012; Pawlowski et al., 2017), ensembles have repeatedly been found to perform best empirically (Lee et al., 2015; Lakshminarayanan et al., 2016). Much of the active literature on ensembles in supervised learning is concerned with computational efficiency, with various proposals for reducing the compute or memory footprint of training and inference on large ensembles (Wen et al., 2020; Zhu et al., 2019; Havasi et al., 2020)

3 BACKGROUND

For clarity of writing, we have interspersed most background information alongside the relevant sections. Throughout this work, we represent Markov Decision Process (MDP) as $M = \langle \mathcal{S}, \mathcal{A}, r, \mathcal{P}, \gamma \rangle$, with state space $\mathcal{S}$, action space $\mathcal{A}$, reward function $r : \mathcal{S} \times \mathcal{A} \to \mathbb{R}$, transition dynamics $\mathcal{P}$, and discount γ. In offline RL, we assume access to a dataset of interactions with the MDP, which we will represent as collection of tuples $D = \{(s, a, s', r, t)\}^N$, where t is an indicator variable that is set to True when s' is a terminal state.

4 METHODOLOGY

Two neural networks with an identical architecture, trained in an identical manner, will make different predictions outside the training set when their weights are initialized with different random draws from the initial weight distribution. So a natural question is, "Which network's predictions can we trust?" An answer to this question can be motivated by referring to the literature of infinite-width networks. When performing mean-squared error regression in the infinite-width regime, informally speaking, an intriguing property is that the distribution of predictions on unseen data is given by a Gaussian Process whose kernel function is solely defined by, 1) the architecture, and 2) the choice of initial weight distribution (Lee et al., 2019). Hence, to leverage the built-in architectural inductive biases of value networks for offline RL, we can train policies to act with respect to the lower-confidence bound (LCB) of the derived Gaussian Process.

In what follows, we present our proposed algorithm, MSG, which leverages ensembles to approximate the LCB. Additionally, using the literature on infinite-width networks, we demonstrate the theoretical advantage of forming ensembles in the manner we propose, which deviates from the current use of ensembles in the reinforcement learning literature.

4.1 MODEL STANDARD-DEVIATION GRADIENTS (MSG)

MSG follows an actor critic setup where in each iteration, we first estimate the Q-values of the current policy, and subsequently optimize the policy through gradient ascent on the lower confidence bound of action value estimates.

Policy Evaluation At the beginning of training, we create an ensemble of N Q-functions by taking N samples from the initial weight distribution. Throughout training, the loss for the Q-functions is the standard least-square Q-evaluation loss,

$$\mathcal{L}(\theta^i) = \mathbb{E}_{(s,a,r,s',t)\sim D}\Big[\big(Q_{\theta^i}(s,a) - y^i(r,s',t,\pi)\big)^2\Big] \tag{1}$$

$$y^i := r + (1-t)\cdot\gamma\cdot\mathbb{E}_{a'\sim\pi(s')}\Big[Q_{\bar{\theta}^i}(s',a')\Big] \tag{2}$$

where $\theta^i, \bar{\theta}^i$ denote the parameters and target network parameters for the ith Q-function, and $t = \mathbb{1}[s' \text{ is terminal}]$. In practice, the expectation in equation 1 is estimated by a minibatch, and the expectation in equation 2 is estimated with a single action sample from the policy. After every update to the Q-function parameters, their corresponding target parameters are updated to be an exponential moving average of the parameters in the standard fashion. **A key factor to note is that, in contrast to the typical usage of ensembles in actor critic algorithms, each ensemble member's update (and y^i) is completely independent from other ensemble members. As we will present below, this an important algorithmic choice, both theoretically (Theorem 5.2) and empirically (section 6.2.2).**

Policy Optimization As described above, the choice of architecture and weight initialization induces a distribution on predictions. Having approximated this distribution using an ensemble of value networks, we can optimize the policy with respect to a lower confidence bound on action values. Specifically, our proposed policy optimization objective in MSG is,

$$\max_{\pi} \mathbb{E}_{s\sim D, a\sim\pi(s)}\Big[\mu(s,a) + \beta \cdot \sigma(s,a)\Big] \quad \text{where} \quad \mu(s,a) = \operatorname*{mean}_i\Big[Q_{\theta^i}(s,a)\Big], \quad \sigma(s,a) = \operatorname*{std}_i\Big[Q_{\theta^i}(s,a)\Big]$$

where $\beta \in \mathbb{R}$ is a hyperparameter that trades off conservatism and optimism. As our problem setting is that of offline RL requiring conservatism, we use $\beta \leq 0$. It is interesting that our proposed objective is in a sense the reverse of the UCB method used for exploration (Auer, 2002).

4.2 The trade-off between trust and pessimism

While our hope is to leverage the distributions induced by the architecture choice, it is not always feasible to do so; designed architectures can still be fundamentally biased in some manner, or simply we can be in a setting with insufficient data coverage Thus we need to trade-off trusting the generalization ability of our models with the pessimistic approach of support constraints. In this work, inspired by CQL (Kumar et al., 2020), we add the following regularizer to our policy evaluation objective (equation 1),

$$\mathcal{R}(\theta^i) = Q_{\theta^i}(s, a^\pi) - Q_{\theta^i}(s, a^D) \tag{3}$$

and control its contribution by weighting the regularization term with weight α. Here a^D denotes the action taken in state s in the dataset, and a^π is a sample from $\pi(s)$. An example scenario where we found this to be necessary is when the offline dataset only contained expert trajectories due to narrow data distributions.

5 Independence in ensembles matters

5.1 The structure of uncertainties depends on how ensembling is done

In the reinforcement learning literature, ensembles are widely used for combatting over-estimation bias (Haarnoja et al., 2018; Fujimoto et al., 2018; 2019; Kumar et al., 2020; Agarwal et al., 2020; Ghasemipour et al., 2021). However, the typical usage of ensembles is to compute a target value y using the ensemble of target networks, and subsequently update all the Q-functions with respect to the same target, typically the minimum over targets. Hence, the objectives for all the Q-functions share the same target value. In this section, drawing upon the literature of infinitely wide networks, we demonstrate that having the updates for ensemble members be independent of one-another – as done in MSG – results in uncertainty estimates that align more closely with intuitive expectations, compared to when their targets are shared.

We study this difference in the setting of policy evaluation using an infinite ensemble of infinite-width Q-function networks (i.e. an ensemble of infinitely many Q-functions, each of which is an infinite-width neural network, with the only difference being that their weights are initialized through independent random draws from the initial weight distribution). For sake of simplicity of derivations we assume that the policy we are trying to evaluate is deterministic and that we do not have terminal states in the MDP. The policy evaluation routine we consider repeatedly performs the following steps,

- **Compute TD Targets** For each $(s, a, r, s') \in D$ compute the TD targets $y^i(r, s', \pi)$

- **Fit the Q-functions** For each ensemble member, optimize the following objective until convergence using full batch gradient descent.

$$\frac{1}{|D|} \sum_{(s,a,r,s') \in D} \left[\left(Q_{\theta^i}(s,a) - y(r,s',\pi) \right)^2 \right] \tag{4}$$

First we establish some notation. Let $\mathcal{X}$ denote a matrix where the rows are the state-action pairs (s,a) in the offline dataset. from the dataset. Let $\mathcal{R}$ be the $|D| \times 1$ matrix containing the rewards observed after each (s,a) in $\mathcal{X}$. Let $\mathcal{X}'$ denote a matrix where the rows are the next state and policy action $(s', \pi(s'))$ Additionally let,

$$\hat{\Theta}_0(A,B) := \nabla_\theta Q_\theta(A) \cdot \nabla_\theta Q_\theta(B)^T|_{t=0} \qquad \hat{\Theta}_0^{-1} := \hat{\Theta}_0(\mathcal{X},\mathcal{X})^{-1} \qquad C := \hat{\Theta}_0(\mathcal{X}',\mathcal{X}) \cdot \hat{\Theta}_0^{-1}$$

$\hat{\Theta}_0(A,B)$ above is referred to as the tangent kernel (Jacot et al., 2018), which is defined as the outerproduct of gradients of the Q-function, at initialization (iteration $t = 0$). The definition of $\hat{\Theta}_0$ does not contain the variable i indexing the ensemble members because, at infinite width, $\hat{\Theta}_0(A,B)$ converges to a deterministic kernel and hence is the same for all ensemble members.

Intuitively, C is a $|D| \times |D|$ matrix where $c_{p,q}$ (the element at row p, column q) is a measure of similarity between $(s', \pi(s'))$ (in the pth row of $\mathcal{X}'$) and (s,a) (in the qth row of $\mathcal{X}$). Let $\mathcal{Y}_t^i$ (with shape $|D| \times 1$) denote the targets used for fitting Q_{θ^i} at iteration t.

Theorem 5.1 *At the end of iteration t we will have,*

$$\begin{aligned}
&Q_{\theta^i}(\mathcal{X}) = \mathcal{Y}_t^i \\
&Q_{\theta^i}(\mathcal{X}') = Q_{\theta^i}(\mathcal{X}')|_{t=0} + C \cdot \left(\mathcal{Y}_t^i - Q_{\theta^i}(\mathcal{X})|_{t=0} \right) \\
&\forall (s,a) \in \mathcal{S} \times \mathcal{A}, Q_{\theta^i}(s,a) = Q_{\theta^i}(s,a)|_{t=0} + \hat{\Theta}_0\Big((s,a),\mathcal{X}\Big) \cdot \hat{\Theta}_0^{-1} \cdot \left(\mathcal{Y}_t^i - Q_{\theta^i}(\mathcal{X})|_{t=0} \right)
\end{aligned}$$

Theorem 5.1 allows us to study the evolution of the ensemble in closed form, which enables us to study the effect of different methods for computing TD targets. Let us consider the difference amongst the following two methods, one where each ensemble member uses its own predictions to compute the TD targets, and one where all ensemble members share the same target:

- **Method 1 (Independent Targets):** $y^i(s,a) = r + \gamma \cdot Q_{\theta^i}(s', \pi(s))$
- **Method 2 (Shared Mean Targets):** $\forall i, y^i(s,a) = r + \gamma \cdot \mathop{\mathbb{E}}_{ensemble}\Big[Q_{\theta^i}(s', \pi(s))\Big]$

Theorem 5.2 *(Informal Intuition) After t iterations, for both methods we have,*

$$\mathop{\mathbb{E}}_{ensemble}\Big[Q_{\theta^i}(s,a)\Big] = \hat{\Theta}_0\Big((s,a),\mathcal{X}\Big) \cdot \hat{\Theta}_0^{-1} \cdot (1 + \ldots + \gamma^t C^t) \cdot \mathcal{R}$$

However, the ensemble variances are very different. *When the targets used are independent (Method 1), $\mathop{\text{Std}}_{ensemble}\Big[Q_{\theta^i}(s,a)\Big]$ contains important additional terms modulated by the matrix, $(1 + \ldots + \gamma^t C^t)$.*

As mentioned above, the matrix C captures a notion of similarity between the (s,a) in $\mathcal{X}$, and the $(s', \pi(s'))$ in $\mathcal{X}'$. Thus, the term C^t has the interpretation of where the policy $\pi(s)$ would find itself t steps into the future, and $(1 + \ldots + \gamma^t C^t)$ can be interpreted as the policy's discounted state-action visitation, but in the feature-space given by the neural network architecture. Since in ensembles the standard deviation of predictions quantifies the amount of uncertainty, **Theorem 5.2 tells us that when the targets are independent, the ensemble of Q-functions "backs up the uncertainties through dynamic programming".**

In contrast, when the targets are shared, the standard deviation of ensemble predictions is only modulated by C, meaning that it is not taking into the account the dynamics of the MDP and the actions of the policy being evaluated. In fact, the uncertainties obtained in this scenario (e.g. Method 2 above) are equivalent to an oracle providing the shared values $\mathcal{Y}_t$, us initializing an ensemble of

Q-functions, and fitting them to regress $\mathcal{Y}_t$ using mean-squared error. Lastly, we note that this phenomenon is not limited to the targets being `Shared Mean`; regardless of what the target values are, if they are shared amongst ensemble members, this collapse of uncertainties will occur. It is interesting that this such differences do not arise in supervised learning, as they are solely due to the recursive dynamic programming nature of policy evaluation.

One aspect that the presented theorems do not touch upon is whether through better choice of shared target values we can approximate a lower-confidence bound (LCB) to the uncertainties of independent ensembles (e.g. computed the targets as "shared min" or "shared mean minus std (LCB)"). We empirically investigate this question in section 6.2.2 and find that they do not lead to effective batch RL algorithms.

5.2 Validating theoretical predictions

In this section we aim to evaluate the validity of our theoretical discussion above in a simple toy MDP that allows us to follow the idealized setting of the presented theorems more closely, and allows for visualization of uncertainties obtained through different ensembling approaches.

Continuous Chain MDP The MDP we consider has state-space $\mathcal{S} = [-1, 1]$, action space $\mathcal{A} \in \mathbb{R}$, deterministic transition dynamics $s' = s + a$ clipped to remain inside $\mathcal{S}$, and reward function $r(s, a) = \mathbb{1}[s' \in [0.75, 1]]$.

Data Collection & Evaluation Policy The offline dataset we generate consists of 40 episodes, each of length 30. At the beginning of each episode we initialize at a random state $s \in \mathcal{S}$. In each step take a random action sampled from Unif$(-0.3, 0.3)$, and record all transitions (s, a, r, s'). For evaluating the uncertainties obtained from different approaches, we create regions of missing data by removing all transitions such that s or s' are in the range $[-0.33, 0.33]$. The policy we choose to evaluate with the different approaches is $\forall s, \pi(s) = 0.1$.

Optimal Desired Form of Uncertainty Note that the evaluation policy $\pi(s) = 0.1$ is always moving towards the positive direction, and there is lack of data for states in the interval $[-0.33, 0.33]$. Hence, what we would expect is that in the region $[0.33, 1]$ there should not be a significant amount of uncertainty, while in the region $[-1, -0.33]$ there should be significantly more uncertainty about the Q-values of π because the policy will be passing through $[-0.33, 0.33]$ where there is no data.

Experiment To evaluate the quality of uncertainties obtained from different Q-function ensembling approaches, we create $N = 64$ Q-function networks, each being a one hidden layer neural network with hidden dimension 512 and `tanh` activation. The initial weight distribution is a fan-in truncated normal distribution with scale 10.0, and the initial bias distribution is fan-in truncated normal distribution with scale 0.05. We did not find results with other activation functions and choices of initial weight and bias distribution to be qualitatively different. The networks are optimized using the Adam (Kingma & Ba, 2014) optimizer with learning rate `1e-4`. In each iteration, we first compute the TD targets using the desired approach (e.g. independent vs. shared targets) and then fit the Q-functions to their respective targets with 2000 steps of full batch gradient descent. We train the networks for 1000 such iterations (for a total of 2000×1000 gradient steps). Note that we do not use target networks. Given the small size of networks and data, these experiments can be done within a few minutes using a single GPU in `Google Colaboratory` which we will also opensource.

Results We visualize and compare the uncertainties obtained when the targets are computed as:

- **Independent:** $y^i = r + \gamma \cdot Q_{\theta^i}(s', \pi(s'))$
- **Independent Double-Q:** $y^i = r + \gamma \cdot \min\Big[Q^1_{\theta^i}(s', \pi(s')), Q^2_{\theta^i}(s', \pi(s'))\Big]$
- **Shared Mean:** $y = r + \gamma \cdot \text{mean}\Big[Q_{\theta^i}(s', \pi(s'))\Big]$
- **Shared LCB:** $y = r + \gamma \cdot \left[\text{mean}\Big[Q_{\theta^i}(s', \pi(s'))\Big] - 2 \cdot \text{std}\Big[Q_{\theta^i}(s', \pi(s'))\Big]\right]$
- **Shared Min:** $y = r + \gamma \cdot \min\Big[Q_{\theta^i}(s', \pi(s'))\Big]$

In Figure 1 we plot the mean and two standard deviations of the predicted values for the policy we evaluated, $\pi(s) = 0.1$. **As predicted by Theorem 5.2, the only setting which matches the desired**

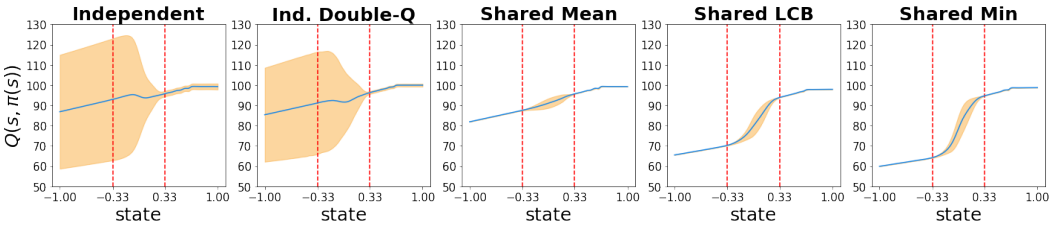

Figure 1: Verifying theoretical predictions on the toy Continuous Chain MDP. The marked interval $[-0.33, 0.33]$ denotes the region of state-space with no data. As anticipated by Theorem **??**, when the value functions are trained independently, the derived uncertainties capture the interaction between available data, the structure of the MDP, the policy being evaluated. When the targets are shared, the derived uncertainties are equivalent to having performed regression for predicting oracle-given values, i.e. there is only some uncertainty between $[-0.33, 0.33]$ because there is no data in that region.

Domain	BC	CQL	α	F-BRC (no bonus)	α	MSG ($N = 64$)	β	α	Data Top 25
halfcheetah-medium	36.1	$\mathbf{50.1 \pm 1.2}$	0	45.7 ± 0.5	0.01	$\mathbf{50.6 \pm 1.5}$	0	0	37.0 ± 2.0
hopper-medium	29.0	90.2 ± 10.5	2.58	$\mathbf{99.0 \pm 4.1}$	0.012	88.2 ± 11.6	-1	0.5	101.1 ± 1.1
walker2d-medium	6.6	$\mathbf{82.8 \pm 0.6}$	3.38	$\mathbf{81.6 \pm 0.2}$	0.016	$\mathbf{83.6 \pm 2.0}$	-1	0.1	77.6 ± 1.4
halfcheetah-mixed	38.4	47.6 ± 2.5	0.67	45.3 ± 0.1	0.01	$\mathbf{52.1 \pm 1.7}$	0	0	38.1 ± 4.1
hopper-mixed	11.8	61.1 ± 36.8	0.67	29.3 ± 0.8	0.019	$\mathbf{82.1 \pm 24.2}$	-2	0	101.8 ± 1.5
walker2d-mixed	11.3	$\mathbf{20.5 \pm 3.8}$	3.38	$\mathbf{28.4 \pm 5.7}$	0.038	$\mathbf{24.0 \pm 9.4}$	-2	0.1	50.6 ± 3.9

Table 1: Results on Gym subset of the D4RL benchmark. CQL, F-BRC, and MSG are tuned with an equal hyperparameter search budget. Running the best found hyperparameter using 5 new random seeds. Each run is evaluated for 10 episodes, and the mean and standard deviation across the 5 runs is reported in the table. For fairness of comparison, F-BRC is ran without adding a survival reward bonus. MSG and CQL are implemented in our code, and for F-BRC we use the opensourced codebase.

form of uncertainties are the "Independent" ensembling mechanism employed in MSG, where each member computes its own TD target and they are not shared[1].

A number of additional observations can be made from Figure 1. First, note that whenever the targets are shared the uncertainties collapse, except when $s \in [-0.33, 0.33]$ since there was no data in this region. **This exactly follows the prediction in Theorem 5.2 that when the targets are shared, the uncertainties are equivalent to the setting of regression on oracle-provided target values; in other words, it does not take into account the transitions dynamics due to following the evaluation policy π.** A second observation following our predictions is that `Shared LCB` and `Shared Min` share the same uncertainty structure as `Shared Mean`. Lastly, although `Shared LCB` and `Shared Min` result in collapse of uncertainty, they do provide a seemingly good approximation to the lower-bound of `Independent` predictions. While our theoretical considerations do not evaluate the suitability of these lower bounds, empirically – as will be shown below – we were unable to train effective policies on offline RL benchmarks using `Shared LCB` and `Shared Min`.

6 Experiments

In this section we seek to empirically answer the following questions: 1) How well does MSG perform compared to current state-of-the-art? 2) Can we match the performance of MSG through efficient ensemble approaches? 3) Are the theoretical differences in ensembling approaches practically relevant?

Domain	CQL (Paper)	MSG ($N = 64$)	β	α
antmaze-umaze	74.0	$\mathbf{96.8 \pm 2.0}$	-8	0.1
antmaze-umaze-diverse	**84.0**	60.2 ± 7.1	-8	0.5
antmaze-medium-play	61.2	$\mathbf{80.0 \pm 9.4}$	-4	0.1
antmaze-medium-diverse	53.7	$\mathbf{78.8 \pm 5.5}$	-4	0.1
antmaze-large-play	15.8	$\mathbf{64.8 \pm 10.7}$	-8	0
antmaze-large-diverse	14.9	$\mathbf{68.8 \pm 11.7}$	-8	0

Table 2: Result on D4RL antmaze domains. As we were unable to reproduce CQL antmaze results, we present the numbers reported by the original paper which uses the same network architectures. We could not understand why antmaze-umaze-diverse had a lower performance than one would expect.

6.1 GYM D4RL BENCHMARK

We begin by evaluating MSG on the Gym (Brockman et al., 2016) subset of the D4RL offline RL benchmark (Fu et al., 2020). The Gym domains are by far the most used subset of the D4RL benchmark in prior work, and are a very valuable setting for validating algorithms. Amongst the different data settings we focus our experiments on the `medium` and `medium-replay` (sometimes referred to as `mixed`) settings as the other data setting could not adequately differentiate between competitive methods. Details such as hyperparameter search procedure are described in Appendix B.

In addition to validating MSG, a secondary objective of ours is to gain a sense for the upper bound of performance for various algorithms on D4RL Gym. For this reason – with an equal hyperparameter tuning budget – we tune the main hyperparameter for each algorithm As can be seen in Table 1, across the board in D4RL Gym, MSG is competitive with very well-tuned current state-of-the-art algorithms. We also note that our results for baseline algorithms exceed prior reported results (often significantly), providing us confidence in their implementation.

Thus far we established the validity of MSG as an offline RL algorithm. However, on the gym domains considered above, MSG's performance is on par with CQL and F-BRC, and does not motivate the use of ensembles in lieu of support constraints. To enable a better comparison amongst competing algorithms, we experiment with the significantly more challenging antmaze tasks.

The antmaze tasks in D4RL, and in particular the two antmaze-large settings, are considered to be extremely challenging. The data for antmaze tasks consists of many episodes of an Ant agent (Brockman et al., 2016) running along arbitrary paths in a maze. The data from these trajectories is relabeled with a reward of 1 when near a particular location in the maze (at which point the episode is terminated), and 0 otherwis The undirected, extremely sparse reward nature of antmaze tasks make them very challenging, especially for the large maze sizes.

Table 2 presents our empirical results. To the best of our knowledge, CQL (Kumar et al., 2019), is considered to be the current state-of-the-art offline RL algorithm on the antmaze tasks and is the method we compare to. As we were unable to reproduce the reported results for CQL, for fairness include the numbers reported by the original work which uses the same network architectures. As can be seen, MSG achieves unprecedented results on the antmaze domains, clearly demonstrating the significant advantage of employing ensembles for batch RL.

6.2 EFFICIENT ENSEMBLES & ENSEMBLE ABLATIONS

In this section we dissect what aspects of MSG contribute to its superior results, and investigate whether the advantages of MSG can be realized through efficient ensemble approximations.

6.2.1 EFFICIENT ENSMEBLES

Thus far we have demonstrated the significant performance gains attainable through MSG. An important concern however, is that of parameter and computational efficiency: "Deep Ensembles" re-

[1]Note that `Independent Double-Q` is still an independent ensemble, where each ensemble member has an architecture containing a min-pooling on top of two subnetworks.

sult in an N-fold increase in memory and compute usage for the Q-networks. While this might not be a significant problem for D4RL benchmark domains due to small model footprints , it becomes a major bottleneck with larger architectures such as those used in language and vision domains. To this end, we evaluate whether recent advances in efficient ensemble approaches also transfer well to the problem of batch RL. Specifically, the efficient ensemble approaches we consider are:

Multi-Input Multi-Output (MIMO) (Havasi et al., 2020) MIMO is an ensembling approach that approximately has the same parameter and computational footprint as a single network. The MIMO approach only modifies the input and output layers of a given network. In MIMO, to compute predictions for data-points $x_1, ..., x_N$ under an ensemble of size N, the data-points are concatenated and passes to the network. The output of the network is then split into N predictions $y_1, ..., y_N$. For added clarification, we include Figure 2a depicting how a MIMO ensemble network functions.

Multi-Head In this ensemble variant, we modify the last layer of a single value network to output N predictions instead of a single Q-value.

Batch Ensembles (Wen et al., 2020) Batch Ensembles incorporate rank-1 modulations to the weights of fully-connected layers. More specifically, let W be the weight matrix of a given fully-connected layer and let x be the input to the layer. The output of the layer for ensemble member i is computed as $\sigma(((W^T(x \circ r^i)) \circ s^i) + b^i)$, where $\circ$ is the element-wise product, parameters with superscript i are separate for each ensemble member, and σ is the activation function. While Batch Ensemble is efficient in terms of number of parameters, in our actor-critic setup its computational cost is on the same order as deep ensembles since for policy updates we need to evaluate each ensemble member separately.

Results As can be seen in Table 3, the performance gains of MSG can to some extent also be realized by efficient ensemble variants. Interestingly, in our experiments the most effective efficient ensemble approach is Multi-Head ensembles, which is not considered to be the most competitive uncertainty estimation technique in the supervised learning literature. Compared to CQL, Multi-Head ensembles continue to be competitive on D4RL gym, and noticeably outperform CQL on antmaze-large tasks. Additionally, training Multi-Head ensembles is the most efficient method, on par with training without ensembling ($N = 1$).

Nonetheless, compared to MSG using deep ensembles, there is a significant performance gap. We believe this observation very clearly motivates future work in developing efficient uncertainty estimation approaches that are better suited to the domain of reinforcement learning. To facilitate this direction of research, in our codebase which will be open-sourced, we also include a complete boilerplate example amenable to drop-in implementation of novel uncertainty-estimation techniques.

6.2.2 Ensemble Ablations

Finally, through the ablations in Table 3 we seek to create a better sense for the various components of MSG.

- Comparing MSG with deep ensembles ($N = 64$), and Multi-Head ensembles ($N = 64$), to no ensembling ($N = 1$) we see very clearly the massive advantage of ensembling.
- Comparing MSG, which uses `Independent` targets, to `Shared LCB` and `Shared Min` we see that the latter non-independent approaches significantly underperform.
- Comparing CQL to $N = 1$ (no ensembling, only CQL-inspired regularizer), we observe that the CQL regularizer tends to be better on Gym domains, and our regularizer may be better on antmaze domains but our results are inconclusive. The advantage of the regularizer we used is significant computationl efficieny due to not using importance sampling.

7 Discussion

Our work has highlighted the significant power of ensembling as a mechanism for uncertainty estimation, with strong results in offline RL. Theoretically, and practically through benchmark experiments, we have demonstrated the critical importance of how ensembling done. An important outstanding direction is how can we design improved efficient ensemble approximations, as we demonstrated that current approaches used in supervised learning – some of which do lead to state-of-the-art for offline RL results – are not nearly as effective as deep ensembles. We hope that this work engenders new efforts from the community of deep network uncertainty estimation researchers whom thus far have not employed offline reinforcement learning domains as a testbed for validating modern uncertainty estimation techniques.

REFERENCES

Rishabh Agarwal, Dale Schuurmans, and Mohammad Norouzi. An optimistic perspective on offline reinforcement learning. In *International Conference on Machine Learning*, pp. 104–114. PMLR, 2020.

Peter Auer. Using confidence bounds for exploitation-exploration trade-offs. *Journal of Machine Learning Research*, 3(Nov):397–422, 2002.

Greg Brockman, Vicki Cheung, Ludwig Pettersson, Jonas Schneider, John Schulman, Jie Tang, and Wojciech Zaremba. Openai gym. *arXiv preprint arXiv:1606.01540*, 2016.

Jacob Buckman, Carles Gelada, and Marc G Bellemare. The importance of pessimism in fixed-dataset policy optimization. *arXiv preprint arXiv:2009.06799*, 2020.

Bo Dai, Ofir Nachum, Yinlam Chow, Lihong Li, Csaba Szepesvári, and Dale Schuurmans. Coindice: Off-policy confidence interval estimation. *arXiv preprint arXiv:2010.11652*, 2020.

Yihao Feng, Tongzheng Ren, Ziyang Tang, and Qiang Liu. Accountable off-policy evaluation with kernel bellman statistics. In *International Conference on Machine Learning*, pp. 3102–3111. PMLR, 2020.

Justin Fu, Aviral Kumar, Ofir Nachum, George Tucker, and Sergey Levine. D4rl: Datasets for deep data-driven reinforcement learning. *arXiv preprint arXiv:2004.07219*, 2020.

Scott Fujimoto and Shixiang Shane Gu. A minimalist approach to offline reinforcement learning. *arXiv preprint arXiv:2106.06860*, 2021.

Scott Fujimoto, Herke Hoof, and David Meger. Addressing function approximation error in actor-critic methods. In *International Conference on Machine Learning*, pp. 1587–1596. PMLR, 2018.

Scott Fujimoto, David Meger, and Doina Precup. Off-policy deep reinforcement learning without exploration. In *International Conference on Machine Learning*, pp. 2052–2062. PMLR, 2019.

Seyed Kamyar Seyed Ghasemipour, Dale Schuurmans, and Shixiang Shane Gu. Emaq: Expected-max q-learning operator for simple yet effective offline and online rl. In *International Conference on Machine Learning*, pp. 3682–3691. PMLR, 2021.

Mohammad Ghavamzadeh, Shie Mannor, Joelle Pineau, and Aviv Tamar. Bayesian reinforcement learning: A survey. *arXiv preprint arXiv:1609.04436*, 2016.

Chuan Guo, Geoff Pleiss, Yu Sun, and Kilian Q Weinberger. On calibration of modern neural networks. In *International Conference on Machine Learning*, pp. 1321–1330. PMLR, 2017.

Tuomas Haarnoja, Aurick Zhou, Kristian Hartikainen, George Tucker, Sehoon Ha, Jie Tan, Vikash Kumar, Henry Zhu, Abhishek Gupta, Pieter Abbeel, et al. Soft actor-critic algorithms and applications. *arXiv preprint arXiv:1812.05905*, 2018.

Marton Havasi, Rodolphe Jenatton, Stanislav Fort, Jeremiah Zhe Liu, Jasper Snoek, Balaji Lakshminarayanan, Andrew M Dai, and Dustin Tran. Training independent subnetworks for robust prediction. *arXiv preprint arXiv:2010.06610*, 2020.

Kaiming He, Xiangyu Zhang, Shaoqing Ren, and Jian Sun. Identity mappings in deep residual networks. In *European conference on computer vision*, pp. 630–645. Springer, 2016.

Arthur Jacot, Franck Gabriel, and Clément Hongler. Neural tangent kernel: Convergence and generalization in neural networks. *arXiv preprint arXiv:1806.07572*, 2018.

Diederik P Kingma and Jimmy Ba. Adam: A method for stochastic optimization. *arXiv preprint arXiv:1412.6980*, 2014.

Ilya Kostrikov and Ofir Nachum. Statistical bootstrapping for uncertainty estimation in off-policy evaluation. *arXiv preprint arXiv:2007.13609*, 2020.

Aviral Kumar, Justin Fu, George Tucker, and Sergey Levine. Stabilizing off-policy q-learning via bootstrapping error reduction. *arXiv preprint arXiv:1906.00949*, 2019.

Aviral Kumar, Aurick Zhou, George Tucker, and Sergey Levine. Conservative q-learning for offline reinforcement learning. *arXiv preprint arXiv:2006.04779*, 2020.

Ilja Kuzborskij, Claire Vernade, Andras Gyorgy, and Csaba Szepesvári. Confident off-policy evaluation and selection through self-normalized importance weighting. In *International Conference on Artificial Intelligence and Statistics*, pp. 640–648. PMLR, 2021.

Balaji Lakshminarayanan, Alexander Pritzel, and Charles Blundell. Simple and scalable predictive uncertainty estimation using deep ensembles. *arXiv preprint arXiv:1612.01474*, 2016.

Tor Lattimore and Csaba Szepesvári. *Bandit algorithms*. Cambridge University Press, 2020.

Jaehoon Lee, Lechao Xiao, Samuel Schoenholz, Yasaman Bahri, Roman Novak, Jascha Sohl-Dickstein, and Jeffrey Pennington. Wide neural networks of any depth evolve as linear models under gradient descent. *Advances in neural information processing systems*, 32:8572–8583, 2019.

Stefan Lee, Senthil Purushwalkam, Michael Cogswell, David Crandall, and Dhruv Batra. Why m heads are better than one: Training a diverse ensemble of deep networks. *arXiv preprint arXiv:1511.06314*, 2015.

Sergey Levine, Aviral Kumar, George Tucker, and Justin Fu. Offline reinforcement learning: Tutorial, review, and perspectives on open problems. *arXiv preprint arXiv:2005.01643*, 2020.

Ping Li, Jinde Cao, and Zidong Wang. Robust impulsive synchronization of coupled delayed neural networks with uncertainties. *Physica A: Statistical Mechanics and its Applications*, 373:261–272, 2007.

Yujia Li, Daniel Tarlow, Marc Brockschmidt, and Richard Zemel. Gated graph sequence neural networks. *arXiv preprint arXiv:1511.05493*, 2015.

Ben Mildenhall, Pratul P Srinivasan, Matthew Tancik, Jonathan T Barron, Ravi Ramamoorthi, and Ren Ng. Nerf: Representing scenes as neural radiance fields for view synthesis. In *European conference on computer vision*, pp. 405–421. Springer, 2020.

Ashvin Nair, Murtaza Dalal, Abhishek Gupta, and Sergey Levine. Awac: Accelerating online reinforcement learning with offline datasets. 2020.

Radford M Neal. *Bayesian learning for neural networks*, volume 118. Springer Science & Business Media, 2012.

Ian Osband, Benjamin Van Roy, Daniel J Russo, Zheng Wen, et al. Deep exploration via randomized value functions. *J. Mach. Learn. Res.*, 20(124):1–62, 2019.

Georg Ostrovski, Marc G Bellemare, Aäron Oord, and Rémi Munos. Count-based exploration with neural density models. In *International conference on machine learning*, pp. 2721–2730. PMLR, 2017.

Yaniv Ovadia, Emily Fertig, Jie Ren, Zachary Nado, David Sculley, Sebastian Nowozin, Joshua V Dillon, Balaji Lakshminarayanan, and Jasper Snoek. Can you trust your model's uncertainty? evaluating predictive uncertainty under dataset shift. *arXiv preprint arXiv:1906.02530*, 2019.

Nick Pawlowski, Andrew Brock, Matthew CH Lee, Martin Rajchl, and Ben Glocker. Implicit weight uncertainty in neural networks. *arXiv preprint arXiv:1711.01297*, 2017.

Xue Bin Peng, Aviral Kumar, Grace Zhang, and Sergey Levine. Advantage-weighted regression: Simple and scalable off-policy reinforcement learning. *arXiv preprint arXiv:1910.00177*, 2019.

Vincent Sitzmann, Julien Martel, Alexander Bergman, David Lindell, and Gordon Wetzstein. Implicit neural representations with periodic activation functions. *Advances in Neural Information Processing Systems*, 33, 2020.

Alexander L Strehl, Lihong Li, and Michael L Littman. Reinforcement learning in finite mdps: Pac analysis. *Journal of Machine Learning Research*, 10(11), 2009.

P. Thomas, G. Theocharous, and M. Ghavamzadeh. High confidence off-policy evaluation. In *Proceedings of the 29th Conference on Artificial Intelligence*, 2015.

Ashish Vaswani, Noam Shazeer, Niki Parmar, Jakob Uszkoreit, Llion Jones, Aidan N Gomez, Łukasz Kaiser, and Illia Polosukhin. Attention is all you need. In *Advances in neural information processing systems*, pp. 5998–6008, 2017.

Ziyu Wang, Alexander Novikov, Konrad Zolna, Jost Tobias Springenberg, Scott Reed, Bobak Shahriari, Noah Siegel, Josh Merel, Caglar Gulcehre, Nicolas Heess, et al. Critic regularized regression. *arXiv preprint arXiv:2006.15134*, 2020.

Yeming Wen, Dustin Tran, and Jimmy Ba. Batchensemble: an alternative approach to efficient ensemble and lifelong learning. *arXiv preprint arXiv:2002.06715*, 2020.

Yifan Wu, George Tucker, and Ofir Nachum. Behavior regularized offline reinforcement learning. *arXiv preprint arXiv:1911.11361*, 2019.

Mengjiao Yang, Bo Dai, Ofir Nachum, George Tucker, and Dale Schuurmans. Offline policy selection under uncertainty. *arXiv preprint arXiv:2012.06919*, 2020.

Shilin Zhu, Xin Dong, and Hao Su. Binary ensemble neural network: More bits per network or more networks per bit? In *Proceedings of the IEEE/CVF Conference on Computer Vision and Pattern Recognition*, pp. 4923–4932, 2019.

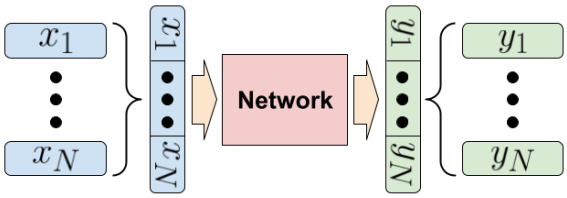

(a) Visual depiction of MIMO Ensemble

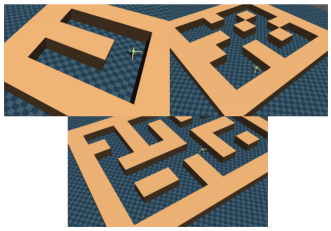

(b) D4RL antmaze tasks. Figure taken from Fu et al. (2020).

A Efficient Ensembles & Ensemble Ablations Table

Domain	CQL	Deep Ens.	MIMO-0.5	MIMO-1	Multi-Head	Batch Ens	$N = 1$	Shared LCB	Shared Min
halfcheetah-medium	50.1	50.6	40.0	44.4	49.8	40.2	48.6	47.9	36.0
hopper-medium	90.2	88.2	60.2	65.1	94.8	41.6	50.2	30.0	43.6
walker2d-medium	82.8	83.6	80.7	83.6	84.5	13.2	84.9	85.5	0.0
halfcheetah-mixed	47.6	52.1	0.0	6.7	49.4	43.0	49.6	51.0	2.3
hopper-mixed	61.1	82.1	22.7	32.5	45.5	35.0	30.5	32.5	6.7
walker2d-mixed	20.5	24.0	14.5	16.8	15.9	12.0	11.5	26.3	0.0
antmaze-large-diverse	15.8	64.8	11.0	26.0	33.5	0.0	noisy 30.5	0.0	0.0
antmaze-large-play	14.9	68.8	7.5	20.5	27.5	0.0	noisy 11.0	0.0	0.0

Table 3: Results for efficient ensembles and ensemble ablations.

B D4RL Gym Details

All policies and Q-functions are a 3 layer neural network with relu activations and hidden layer size 256. The policy output is a normal distribution that is squashed to $[-1, 1]$ using the tanh function. All methods were trained for 1M steps. CQL and MSG are trained with behavioral cloning (BC) for the first 50K steps. F-BRC pretrains with 1M steps of BC.

B.1 Hyperparameter Search

For all methods we performed hyperparameter search using 2 seeds, and for the final choice of hyperparameter ran experiments with 5 new random seed.

MSG $\beta \in \{0., -1., -2., -4. - 8.\}, \alpha \in \{0., 0.1, 0.5, 1., 2.\}$

CQL $\alpha \in \{0., 0.1\} + np.exp(np.linspace(np.log(0.1), np.log(10.), steps = 23))$

F-BRC $\alpha \in \{0.\} + np.exp(np.linspace(np.log(0.01), np.log(10.0), steps = 24))$

C Antmaze Details

We use the same hyperparameter search procedure as Gym results, with same architectures. The only difference is that models are trained for 2M steps and at evaluation time they are rolled out for 100 episodes instead of 10.

In prior work, the rewards in the offline dataset are converted using the formula $4(r - 0.5)$. We also use the same reward transformation.

D THEORY

For our notation to match Lee et al. (2019), throughout this section we use the f to denote the network Q, and we use x instead of (s, a).

In Lee et al. (2019) it is shown that when training an infinitely wide neural network to perform regression using mean squared error, subject to technical conditions on the learning rate used, the predictions of the trained network are equivalent to if we had linearized (Taylor expanded) the network at its initialization, and performed trained the linearized network instead. This means that after t iterations of our policy evaluation procedure, $\forall x, t, \quad f_t^{\text{lin}}(x) = f_t(x)$. Hence we only need to study the evolution of the linearized network f^{lin}.

The theorems in the main manuscript are direct corollaries of the following two derivations.

D.1 EACH HAVE THEIR OWN TARGET

For a single – infinitely wide – ensemble member, using the equations in Lee et al. (2019) (section 2.2, equations 9-10-11) we can write the following recursive updates for our policy evaluation procedure

$$\hat{\Theta}_0^{-1} := \hat{\Theta}_0(\mathcal{X}, \mathcal{X})^{-1} \tag{5}$$

$$C := \hat{\Theta}_0(\mathcal{X}', \mathcal{X})\hat{\Theta}_0^{-1} \tag{6}$$

$$f_{t+1}^{\text{lin}}(\mathcal{X}) = \mathcal{Y}_t \tag{7}$$

$$= \mathcal{R} + \gamma f_t^{\text{lin}}(\mathcal{X}') \tag{8}$$

$$\forall x, f_{t+1}^{\text{lin}}(x) = f_0(x) + \hat{\Theta}_0(x, \mathcal{X})\hat{\Theta}_0^{-1}(\mathcal{Y}_t - f_0(\mathcal{X})) \tag{9}$$

$$\mathcal{Y}_{t+1} = \mathcal{R} + \gamma f_t^{\text{lin}}(\mathcal{X}') \tag{10}$$

$$f_{t+1}^{\text{lin}}(\mathcal{X}') = f_0(\mathcal{X}') + \hat{\Theta}_0(\mathcal{X}', \mathcal{X})\hat{\Theta}_0^{-1}(\mathcal{Y}_t - f_0(\mathcal{X})) \tag{11}$$

$$= f_0(\mathcal{X}') + \hat{\Theta}_0(\mathcal{X}', \mathcal{X})\hat{\Theta}_0^{-1}(\mathcal{R} + \gamma f_t^{\text{lin}}(\mathcal{X}') - f_0(\mathcal{X})) \tag{12}$$

$$= f_0(\mathcal{X}') + C\mathcal{R} + \gamma C f_t^{\text{lin}}(\mathcal{X}') - C f_0(\mathcal{X}) \tag{13}$$

$$= f_0(\mathcal{X}') + C\mathcal{R} - C f_0(\mathcal{X}) + \gamma C f_t^{\text{lin}}(\mathcal{X}') \tag{14}$$

$$= \dots \tag{15}$$

$$= (1 + \ldots + \gamma^t C^t)\Big(f_0(\mathcal{X}') + C\mathcal{R} - C f_0(\mathcal{X})\Big) + (\gamma C)^{t+1} f_0(\mathcal{X}') \tag{16}$$

In the infinite-width regime, the above equations imply the following distributions,

$$\mathop{\mathbb{E}}_{ensemble}[\mathcal{Y}_t] = (1 + \ldots + \gamma^t C^t)\mathcal{R} \tag{17}$$

$$\forall x, \mathop{\mathbb{E}}_{ensemble}[f_{t+1}^{\text{lin}}(x)] = (1 + \ldots + \gamma^t C^t)C\mathcal{R} \tag{18}$$

In addition to the formulae for the expectations above, a key observation from equation 16 to note is that the variance/covariance of terms of interest is modulated by this expression:

$$(1 + \ldots + \gamma^t C^t) \tag{19}$$

This means that the uncertainty being "backed-up/accumulated" through dynamic programming.

D.2 THEY ALL SHARE THE TARGET

Let us consider the setting where all ensemble memebers use their mean as the target.

$$\hat{\Theta}_0^{-1} := \hat{\Theta}_0(\mathcal{X}, \mathcal{X})^{-1} \tag{20}$$

$$C := \hat{\Theta}_0(\mathcal{X}', \mathcal{X})\hat{\Theta}_0^{-1} \tag{21}$$

$$\forall x, f_{t+1}^{\text{lin}}(x) = f_0(x) + \hat{\Theta}_0(x, \mathcal{X})\hat{\Theta}_0^{-1}(\mathcal{Y}_t - f_0(\mathcal{X})) \tag{22}$$

$$\mathcal{Y}_{t+1} = \mathcal{R} + \gamma \mathop{\mathbb{E}}_{ensemble}[f_t^{\text{lin}}(\mathcal{X}')] \tag{23}$$

$$= \mathcal{R} + \gamma C \mathcal{Y}_t \tag{24}$$

$$= \dots \tag{25}$$

$$= (1 + \ldots + \gamma^{t+1}C^{t+1})\mathcal{R} + \mathbb{E}[\gamma^{t+2}C^{t+1}f_0(\mathcal{X}')] \tag{26}$$

$$= (1 + \ldots + \gamma^{t+1}C^{t+1})\mathcal{R} \tag{27}$$

$$f_{t+1}^{\text{lin}}(\mathcal{X}) = \mathcal{Y}_t \tag{28}$$

$$\forall x, f_{t+1}^{\text{lin}}(x) = f_0(x) + C\Big((1 + \ldots + \gamma^t C^t)\mathcal{R} - f_0(\mathcal{X})\Big) \tag{29}$$

In the infinite-width regime, the above equations imply the following distributions,

$$\mathop{\mathbb{E}}_{ensemble}[\mathcal{Y}_t] = (1 + \ldots + \gamma^t C^t)\mathcal{R} \tag{30}$$

$$\forall x, \mathop{\mathbb{E}}_{ensemble}[f_{t+1}^{\text{lin}}(x)] = (1 + \ldots + \gamma^t C^t)C\mathcal{R} \tag{31}$$

As we can see, **the expectation of the learned values is identical** to the previous case where targets were independent. **However, the variance/covariance is completely different.** This key difference arises from the difference between equations 16 and 29. In the setting where the target was shared, the covariance was modulated by the term $(1 + \ldots + \gamma^t C^t)$. However, in the case where the target is the mean, there is no such modulation of the covariance. **The uncertainties obtained with mean targets identical to regressing the uncertainties obtained by regressing $\mathcal{Y}_t$ using an ensemble.**